SUPPORTING INFORMATION

Chinese Journal of Structural Chemistry

Interfacial Engineering of NiFeP/NiFe-LDH Heterojunction for Efficient Overall Water Splitting

Xuanyu Long[1], Jiazhi Meng[1], Jiabao Gu[1], Lanqing Ling[1], Qianwen Li[1], Nan Liu[1], Kaiwen Wang[2]* and Zequan Li[1]*

[1]*The School of Chemistry and Chemical Engineering, Chongqing University, Chongqing 400044, China*
[2]*Beijing Key Lab of Microstructure and Properties of Advanced Materials, Beijing University of Technology, Beijing 100124, China*

Corresponding authors. E-mails: 18811419320@163.com and lzq0313@cqu.edu.cn

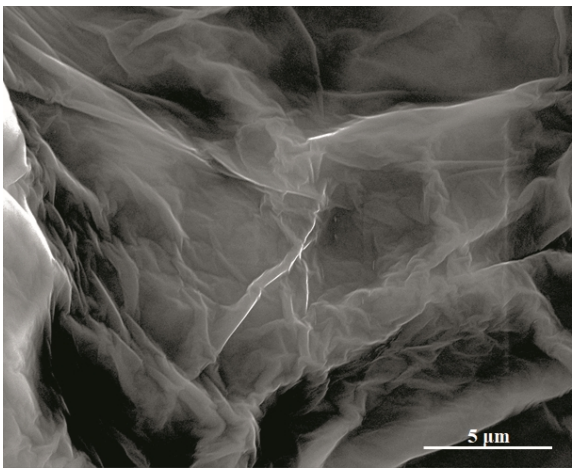

Figure S1. SEM image of graphene oxide (GO).

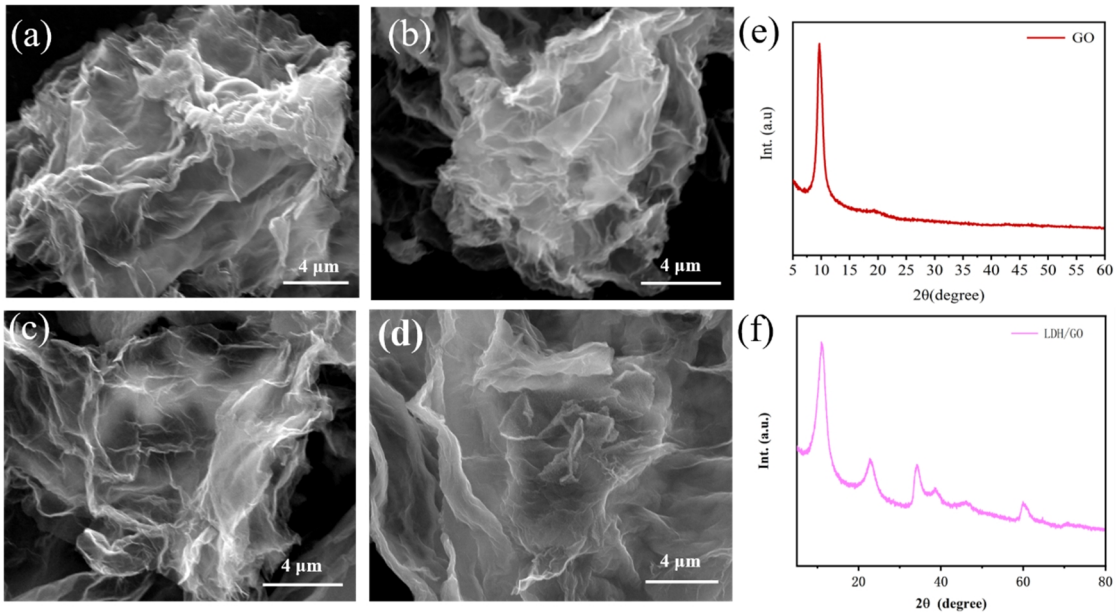

Figure S2. SEM images of the flower-like Ni_xFe_y-LDH/GO: (a) x:y = 0.6:0.4; (b) x:y = 0.8:0.2; (c) x:y = 0.7:0.3; (d) x:y = 0.5:0.5. (e) XRD of GO; (f) XRD of LDH/GO.

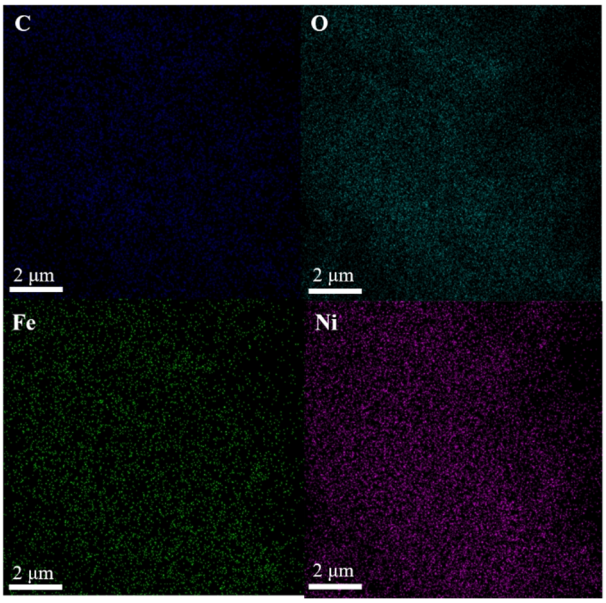

Figure S3. EDS mapping patterns of $Ni_{0.7}Fe_{0.3}$-LDH/GO.

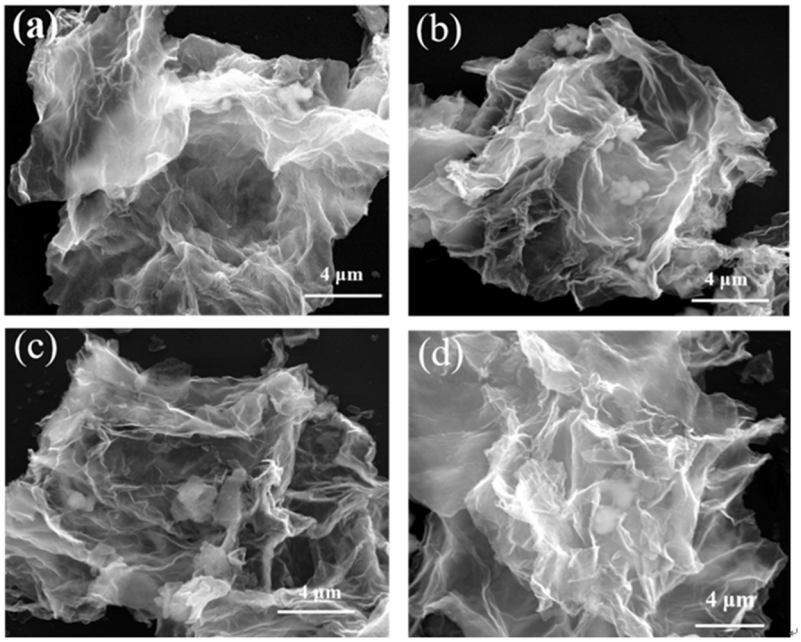

Figure S4. SEM images of the Ni_xFe_yP/LDH/GO: (a) x:y = 0.6:0 4; (b) x:y = 0.8:0.2; (c) x:y = 0.7:0.3; (d) x:y = 0.5:0.5.

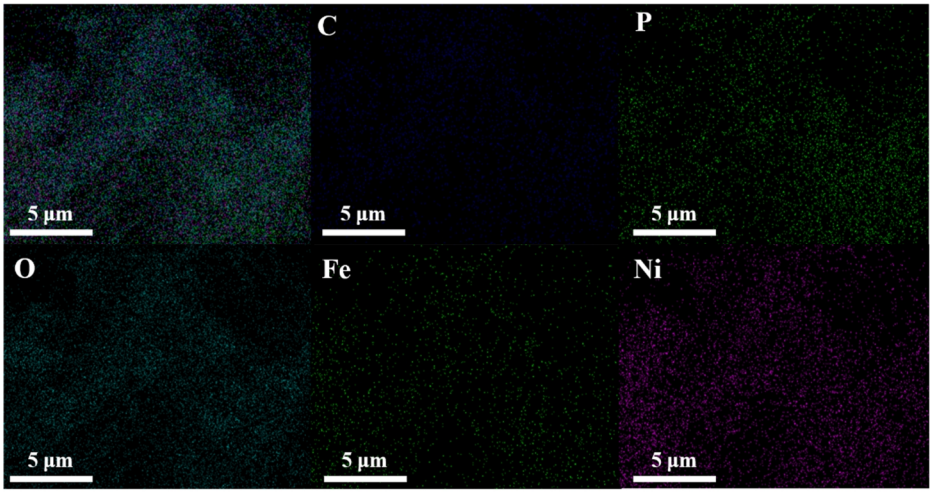

Figure S5. EDS mapping patterns of the flower-like $Ni_{0.7}Fe_{0.3}$P/LDH/GO.

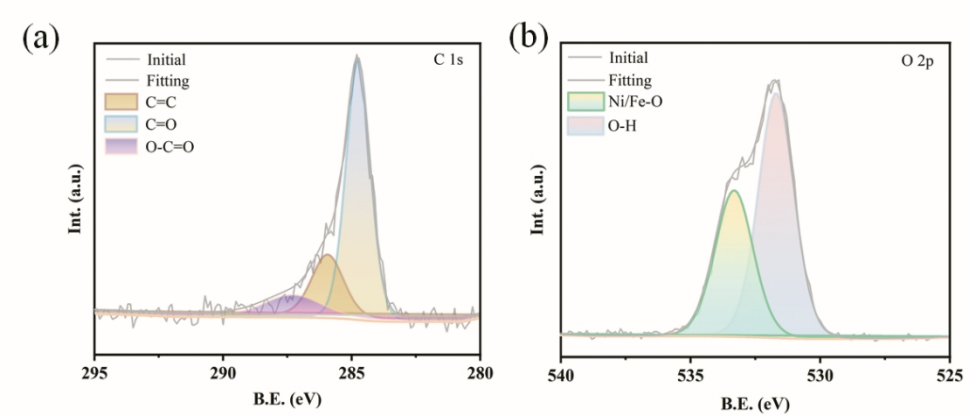

Figure S6. The XPS measurement results for $Ni_{0.7}Fe_{0.3}$P/LDH/GO: (a) C 1*s*, (b) O 2*p* core levels.

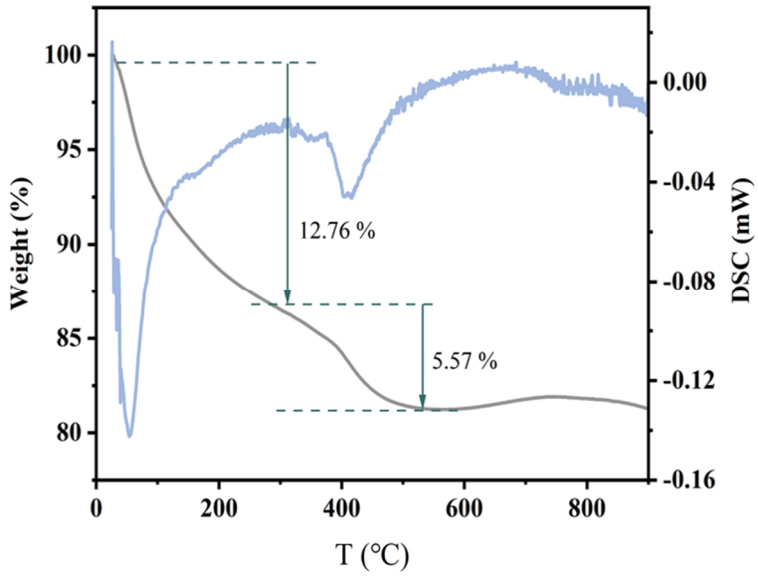

Figure S7. TG analysis of $Ni_{0.7}Fe_{0.3}P$/LDH/GO.

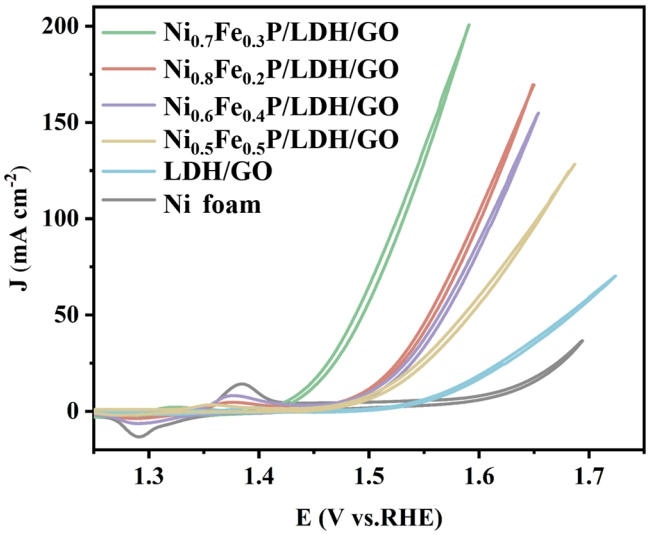

Figure S8. Cyclic voltammetry curves of samples for OER in 1 M KOH at a scan rate of 1 mV·s^{-1} without stirring.

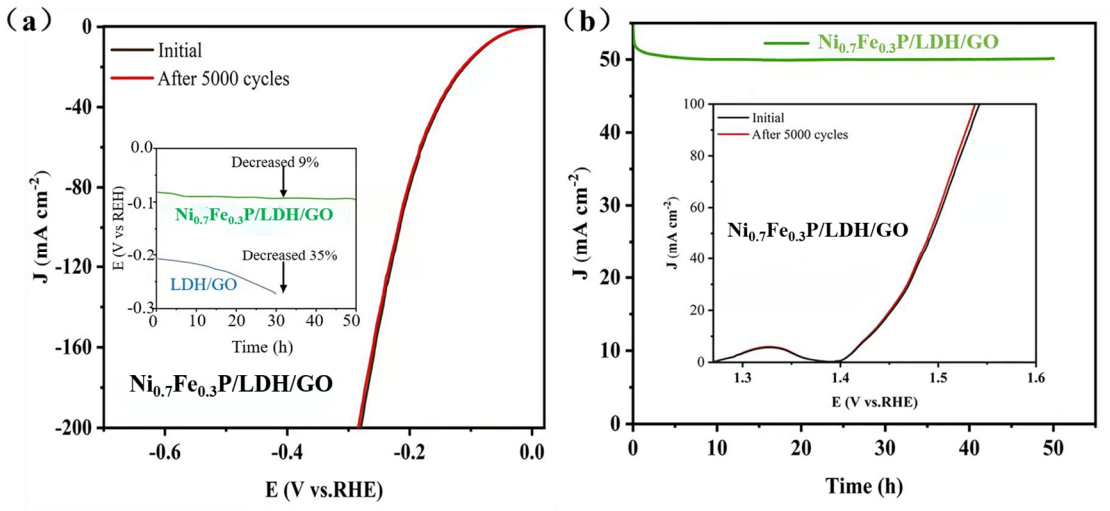

Figure S9. (a) Polarization curves of $Ni_{0.7}Fe_{0.3}P$/LDH/GO before and after 5000 cycles for HER (Inset: The galvanostatic tests of $Ni_{0.7}Fe_{0.3}P$/LDH/GO and LDH/GO are conducted for HER in 1 M KOH at j = 10 mA·cm^{-2}); (b) The constant voltage test of $Ni_{0.7}Fe_{0.3}P$/LDH/GO for OER in 1 M KOH at E = 1.49 V vs. RHE (Inset: polarization curves of $Ni_{0.7}Fe_{0.3}P$/LDH/GO before and after 5000 cycles for OER).

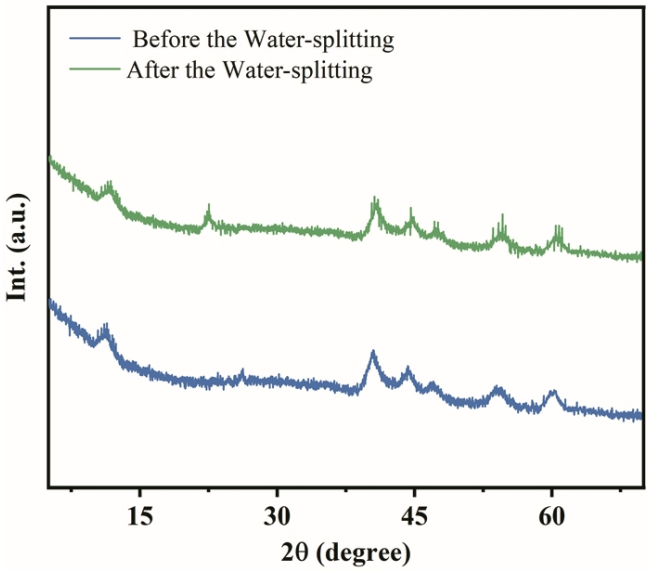

Figure S10. XRD patterns of $Ni_{0.7}Fe_{0.3}P$/LDH/GO before and after overall water splitting.

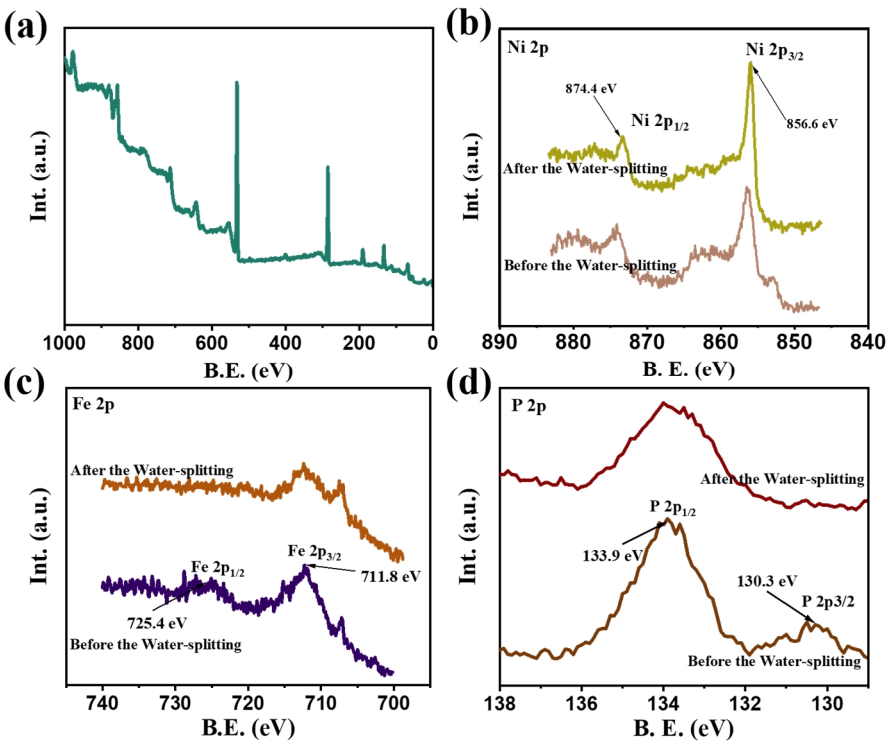

Figure S11. XPS patterns of $Ni_{0.7}Fe_{0.3}P$/LDH/GO before and after overall water: (a) survey, (b) Ni 2*p*, (c) Fe 2*p*, (d) P 2*p* core levels.

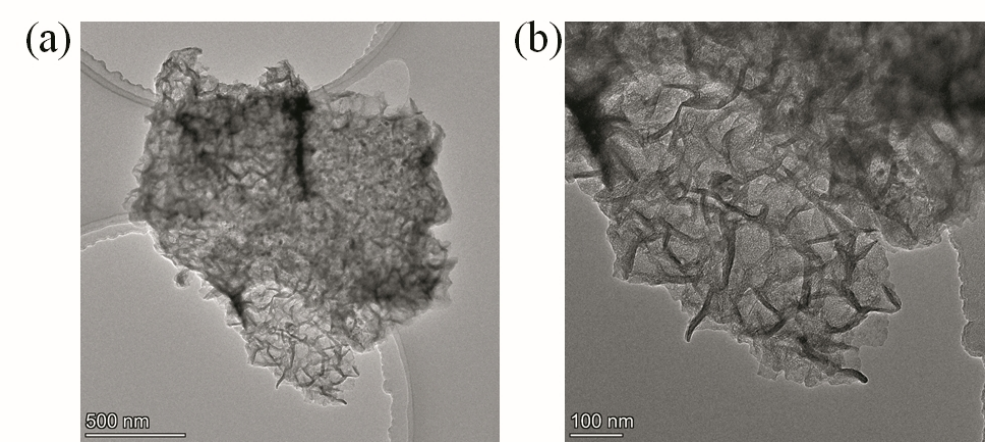

Figure S12. TEM of $Ni_{0.7}Fe_{0.3}P$/LDH/GO after overall water splitting.

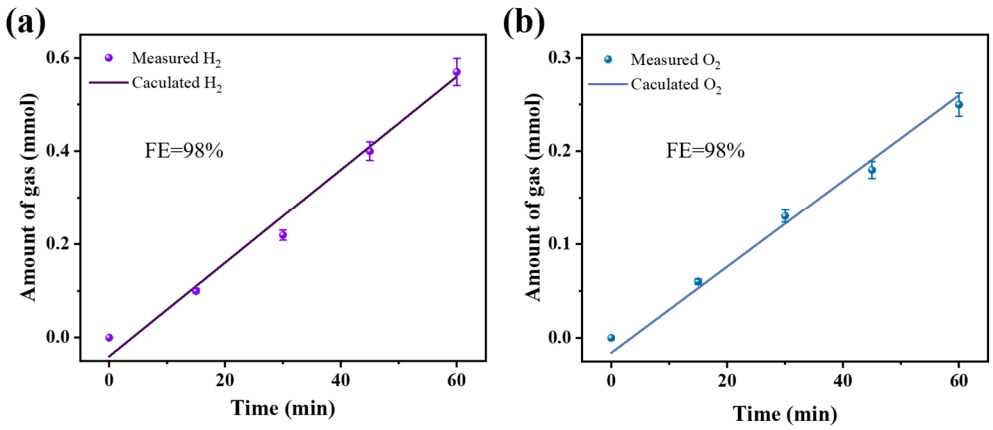

Figure S13. The amount of gas theoretically calculated and experimentally measured vs. time for $Ni_{0.7}Fe_{0.3}P$/LDH/GO: (a) for HER, (b) for OER in 1 M KOH at η = 296 mV vs. theoretically calculated quantities assuming 100% FE for both HER and OER.

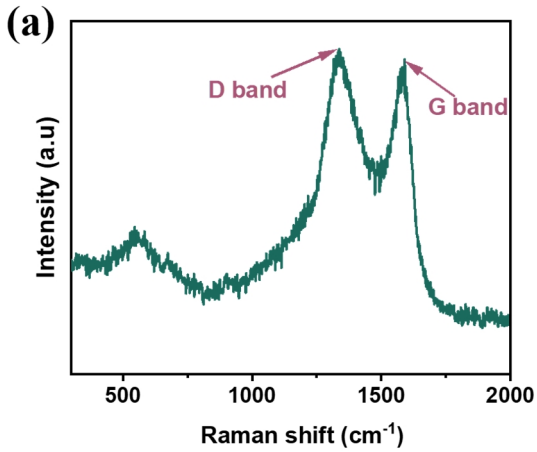

Figure S14. Raman spectra analysis of $Ni_{0.7}Fe_{0.3}P$/LDH/GO.

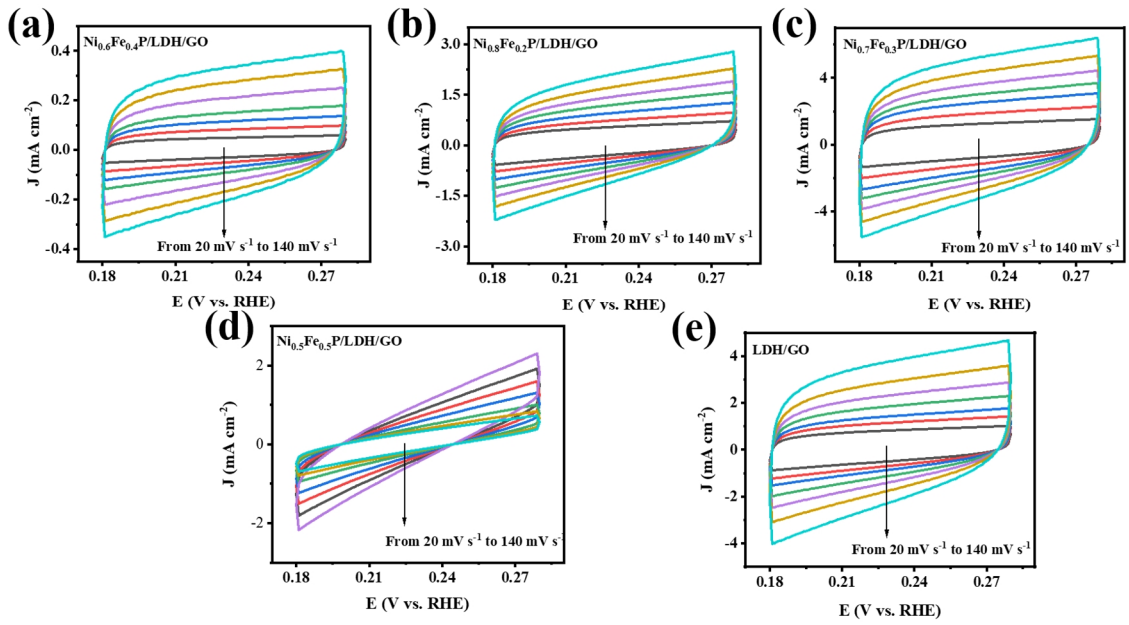

Figure S15. (a–e) cyclic voltammetry (CV) measurement with varied scan rates (20, 40, 60 etc. mV·s^{-1}) for Ni_xFe_yP/LDH/GO under different scan rates in the potential region from 0.18 to 0.28 V vs. RHE

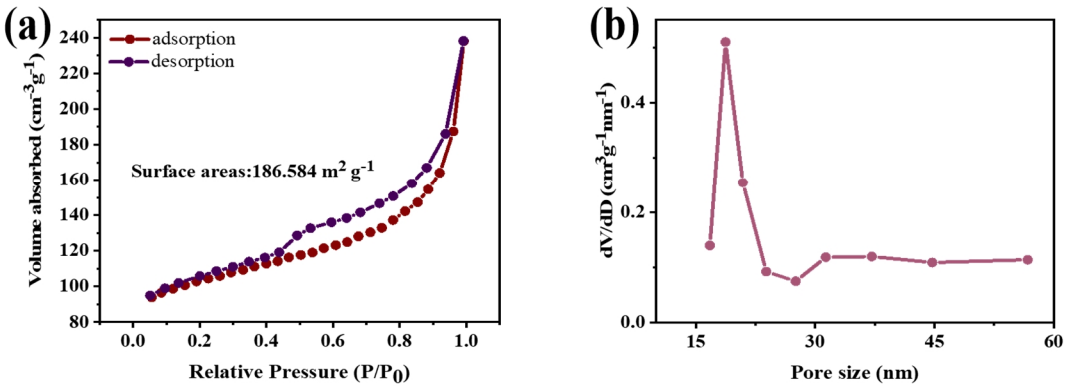

Figure S16. Structural characterization patterns of $Ni_{0.7}Fe_{0.3}P$/LDH/GO: (a) The nitrogen adsorption-desorption isotherm, (b) The pore size distribution result.

Table S1. Inductive Coupled Plasma Emission Spectrometer (ICP-MS) Analysis of Ni_xFe_yP/LDH/GO Heterojunction with Different Ni/Fe Molar Ratios.

Materials	Fe (g)	Ni (g)	Ni/Fe (molar ratios)
$Ni_{0.6}Fe_{0.4}P$/LDH/GO	0.358	0.562	0.592:0.378
$Ni_{0.8}Fe_{0.2}P$/LDH/GO	0.129	0.518	0.883:0.231
$Ni_{0.7}Fe_{0.3}P$/LDH/GO	0.182	0.425	0.724:0.325
$Ni_{0.5}Fe_{0.5}P$/LDH/GO	0.287	0.291	0.496:0.512

Table S2. Inductively Coupled Plasma Optical Emission Spectrometry (ICP-OES) Analysis of $Ni_{0.7}Fe_{0.3}P$/LDH/GO Heterojunction before and after Etching for 20 s.

Materials	Fe (atomic fraction %)	Ni (atomic fraction %)	P (atomic fraction %)
Pristine	23.4	51.8	14.6
Etched	23.7	52.1	1.7

Table S3. Comparison of the Water Splitting Property of $Ni_{0.7}Fe_{0.3}P$/LDH/GO to Other Catalysis in 1 M KOH (j_{10} = 10 mA·cm^{-2})

Catalyst	Overpotential for HER (mV)	Overpotential for OER (mV)	Cell voltage (V)	Stability (h)	References
$Ni_{0.7}Fe_{0.3}P$/LDH/GO	79	198	1.526	25	This work
$Co_3S_4@MoS_2$	136	280	1.58	10	2
$MoO_2@MoS_2@Co_9S_8$	160	310	1.62	20	3
NG-NiFe@MoC_2	150	320	1.53	10	4
Co-P films	94	345	1.56	24	5
Ni/NiP	130	270	1.61	24	6
Al, Fe codoped CoP/RGO	145	280	1.66	10	7
$NiCo_2O_4@Ni_2P$/NAs	141	350	1.52	6	8
NP-RuO_2	87	250	1.62	12	9
NiCoP/CNTs	82	250	1.558	20	10
$NiCo_2O_4$@C	109	220	1.608	48	11
FeCo/CFPs	163	283	1.68	10	12
CoNi-OOH	210	279	1.76	60	13
NiFe@C	195	274	1.63	20	14
$Ni_{1-x}Fe_x$-HP	215	280	1.57	24	15
NiO	424	370	1.6	6	16

n REFERENCES

(1) Hummers, W. O. R. Preparation of graphitic oxide. *J. Am. Chem. Soc*. **1985**, 80, 1339.

(2) Guo, Y.; Tang, J.; Wang, Z.; Kang, Y. M.; Bando, Y.; Yamauchi, Y. Elaborately assembled core-shell structured metal sulfides as a bifunctional catalyst for highly efficient electrochemical overall water splitting. *Nano Energy* **2018**, 47, 494–502.

(3) Li, Y.; Wang, C.; Cui, M.; Xiong, J.; Mi, L.; Chen, S. Heterostructured MoO_2@MoS_2@Co_9S_8 nanorods as high efficiency bifunctional electrocatalyst for overall water splitting. *Appl. Surf. Sci*. **2021**, 543, 148804.

(4) Hu, Q.; Liu, X.; Zhu, B.; Fan, L.; Chai, X.; Zhang, Q.; Liu, J.; He, C.; Lin, Z. Crafting MoC_2-doped bimetallic alloy nanoparticles encapsulated within N-doped graphene as roust bifunctional electrocatalysts for overall water splitting. *Nano Energy* **2018**, 50, 212–219.

(5) Jiang, N.; You, B.; Sheng, M.; Sun, Y. Electrodeposited cobalt-phosphorous-derived films as competent bifunctional catalysts for overall water splitting. *Angew. Chem. Int. Ed.* **2015**, 54, 6251–6254.

(6) Chen, G. F.; Ma, T. Y.; Liu, Z. Q.; Li, N.; Su, Y. Z.; Davey, K.; Qiao, S. Z. Efficient and stable bifunctional electrocatalysts Ni/Ni_xM_y (M = P, S) for overall water splitting. *Adv. Funct. Mater.* **2016**, 26, 3314–3323.

(7) Zai, S. F.; Zhou, Y. T.; Yang, C. C.; Jiang, Q. Al, Fe-codoped CoP nanoparticles anchored on reduced graphene oxide as bifunctional catalysts to enhance overall water splitting. *Chem. Eng. J.* **2021**, 421, 127856.

(8) Wang, Q.; Wang, H.; Cheng, X.; Fritz, M.; Wang, D.; Li, H.; Bund, A.; Chen, G.; Schaaf, P. $NiCo_2O_4$@Ni_2P nanorods grown on nickel nanorod arrays as a bifunctional catalyst for efficient overall water splitting. *Mater. Today Energy* **2020**, 17, 100490.

(9) Cong, N.; Han, Y.; Tan, L.; Zhai, C.; Chen, H.; Han, J.; Fang, H.; Zhou, X.; Zhu, Y.; Ren, Z. Nanoporous RuO_2 characterized by $RuO(OH)_2$ surface phase as an efficient bifunctional catalyst for overall water splitting in alkaline solution. *J. Electroanal. Chem*. **2021**, 881, 114955.

(10) Bian, J. Z.; Song, Z. Y.; Zhang, Y. Z.; Cheng, C. W. NiCoP nanopeapods embedded in carbon nanotube arrays as bifunctional catalysts for efficient overall water splitting. *Mater. Today Nano*. **2019**, 8, 100053.

(11) Deng, J.; Zhang, H.; Zhang, Y.; Luo, P.; Liu, L.; Wang, Y. Striking hierarchical urchin-like peapoded $NiCo_2O_4$@C as advanced bifunctional electrocatalyst for overall water splitting. *J. Power Sources* **2017**, 372, 46–53.

(12) Liu, W.; Du, K.; Liu, L.; Zhang, J.; Zhu, Z.; Shao, Y.; Li, M. One-step electroreductively deposited iron-cobalt composite films as efficient bifunctional electrocatalysts for overall water splitting. *Nano Energy* **2017**, 38, 576–584.

(13) Yu, C.; Lu, J.; Luo, L.; Xu, F.; Shen, P. K.; Tsiakaras, P.; Yin, S. Bifunctional catalysts for overall water splitting: CoNi oxyhydroxide nanosheets electrodeposited on titanium sheets. *Electrochim. Acta* **2019**, 301, 449–457.

(14) Park, S. W.; Kim, I.; Oh, S. I.; Kim, J. C.; Kim, D. W. Carbon-encapsulated NiFe nanoparticles as a bifunctional electrocatalyst for high-efficiency overall water splitting. *J. Catal.* **2018**, 366, 266–274.

(15) Qiao, H.; Yang, Y.; Dai, X.; Zhao, H.; Yong, J.; Yu, L.; Luan, X.; Cui, M.; Zhang, X.; Huang, X. Amorphous (Fe)Ni-MOF-derived hollow (bi)metal/oxide@N-graphene polyhedron as effectively bifunctional catalysts in overall alkaline water splitting. *Electrochim. Acta* **2019**, 318, 430–439.

(16) Mondal, A.; Paul, A.; Srivastava, D. N.; Panda, A. B. NiO hollow microspheres as efficient bifunctional electrocatalysts for overall water-splitting. *Int. J. Hydrogen Energy* **2018**, 43, 21665–21674.